Journal of Organometallic Chemistry, 407 (1991) 107–113
Elsevier Sequoia S.A., Lausanne
JOM 21419

The crystal structure of 1,1′-(1,4,10,13-tetraoxa-7,16-diazacyclooctadecane-7,16-diyldicarbonyl)ruthenocene

C. Dennis Hall *, Adrian W. Parkins, Stanley C. Nyburg and Nelson W. Sharpe
Department of Chemistry, King's College, University of London, Strand, London WC2R 2LS (UK)

(Received September 21st, 1990)

Abstract

The crystal and molecular structure of the ruthenocene-containing cryptand 1,1′-(1,4,10,13-tetraoxa-7,16-diazacyclooctadecane-7,16-diyldicarbonyl)ruthenocene has been determined. The ruthenocene rings are separated by 3.62(1) Å, rotated from eclipsed by ca. 2° and are almost parallel with dihedral angle 1.1(4)°. The carbonyl substituents are *trans* with substitution at the ruthenocene rings staggered by 73.7°.

A growing body of literature is appearing concerning the structures of redox-active ionophores containing a metallocene unit [1–6]. This paper reports on the structure of a redox-active cryptand containing the ruthenocene unit, which was characterised by X-ray crystallography. The overall molecular structure of the title

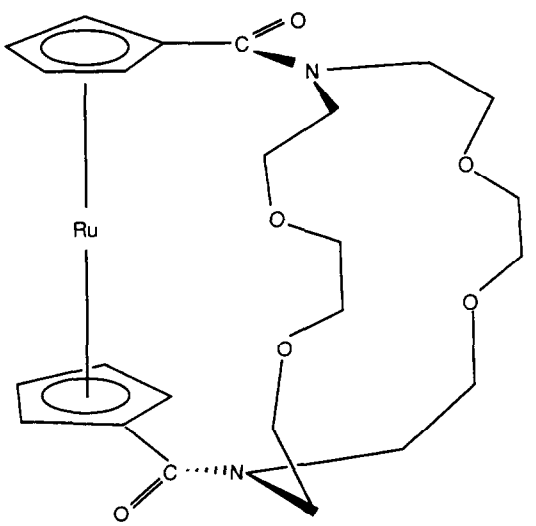

Fig. 1. Schematic representation of the structure of **1**.

0022-328X/91/$03.50

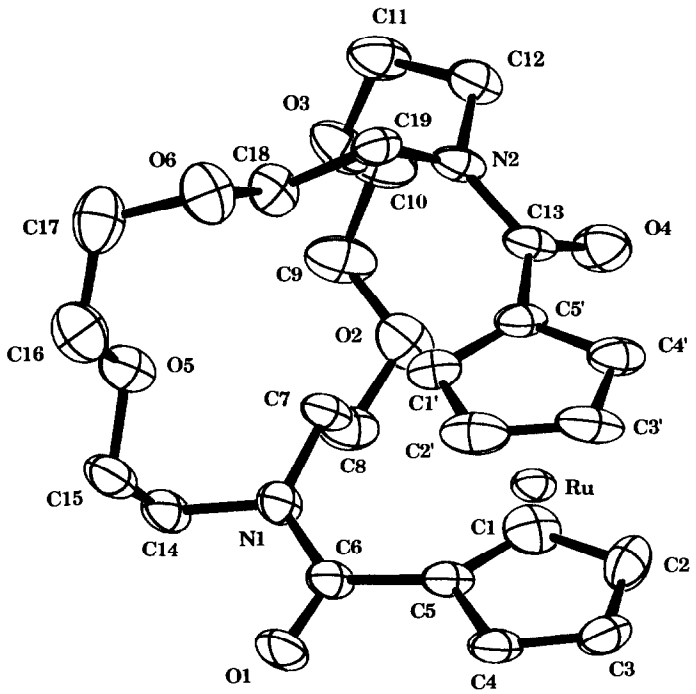

Fig. 2. ORTEP plot of the molecular structure of **1**. (Note; the atom numbering scheme is the same as that employed for the ferrocene analogue reported earlier [3], thus permitting direct comparison. However, the scheme differs from that employed in the NMR study of **1** [7].)

compound (**1**), see Figs. 1 and 2, is best summarised as a cryptand in which the nitrogen atoms are bridged by two polyether chains of equal length and by a ruthenocene unit which is bonded via amido carbonyl substitution at each cyclopentadienyl (Cp) ring. The compound **1** is the ruthenium analogue of a ferrocene-containing cryptand, the structure of which is known [3]. As predicted by earlier NMR studies [7], the two molecules have similar structures, except that: (a) as expected, the separation between the metallocene Cp rings is greater for the ruthenium analogue and (b) the ferrocene analogue crystallises as a dihydrate and its crystal structure contains evidence for H-bonding.

Experimental

Preparative details

The title compound, **1**, was prepared and purified in the manner described previously [7]. The crystal was grown from a solution of **1** in toluene, (ca. 10^{-2} M), in a sealed tube at $-20\,^{\circ}$C. The pale yellow crystals formed as long needles, one of which was cut to the appropriate dimensions, ca. $(0.5\ \text{mm})^3$. The crystals are unstable to air, having a tendency to crumble over 24 h to a primrose powder, although no chemical changes are apparent. The crystal was therefore glued with epoxy resin to the side of a sealed Lindemann glass capillary, under which conditions the crystal retains its integrity indefinitely. However, this precluded precise measurement of crystal dimensions.

Crystal data and structure analysis

For **1**: $C_{24}H_{32}N_2O_6Ru$, $M = 545.6$, monoclinic, $P2_1/n$, $a = 13.702(6)$, $b = 17.919(5)$, $c = 9.413(9)$ Å, $\beta = 81.59(6)°$, $U = 2286.3$ Å^3, $Z = 4$, $D_c = 1{,}58$ g cm^{-3}. The crystal data were collected on a Picker four-circle diffractometer recently interfaced to an AT-TURBO 286 IBM-compatible microcomputer using Ni-filtered Cu-K_α radiation and pulse height analysis. $T = 295$ K, $5 < 2\theta < 100°$, $R(R_w) = 3.8$ (4.6)% for 2159 unique reflections with $I_{(net)} > 2.5\sigma I_{(net)}$. The ruthenium atom was located from the Patterson function and the structure refined by full matrix least squares uising the NRCVAX package [9]. All the H-atoms were found, but calculated positions were used in the refinement (C–H = 1.0 Å). All non-hydrogen atoms were refined anisotropically and the hydrogen atoms were refined with isotropic temperature factors equivalent to those of the atoms to which they are bonded. Atomic coordinates and thermal parameters are listed in Table 1. For non-hydrogen atoms

Table 1

Fractional atomic coordinates and equivalent isotropic temperature factors

Atom	x	y	z	B_{iso} (Å^2)
Ru	0.18392(4)	0.07759(3)	1.03209(6)	2.43(3)
C1	0.3165(5)	0.0747(5)	1.1365(9)	3.5(4)
C2	0.2357(6)	0.0440(5)	1.2315(9)	3.8(4)
C3	0.2019(5)	−0.0204(4)	1.1656(9)	3.4(4)
C4	0.2595(5)	−0.0297(4)	1.0301(9)	3.3(4)
C5	0.3309(5)	0.0300(4)	1.0080(8)	2.7(4)
C1′	0.1633(6)	0.1469(4)	0.8487(8)	3.3(4)
C2′	0.0933(7)	0.0888(4)	0.8613(10)	4.2(4)
C3′	0.0307(6)	0.0961(4)	1.0022(10)	4.0(5)
C4′	0.0638(5)	0.1581(4)	1.0715(9)	3.4(4)
C5′	0.1456(5)	0.1907(4)	0.9776(8)	2.8(4)
C6	0.4025(5)	0.0308(4)	0.8696(8)	2.8(4)
C7	0.4493(5)	0.1664(4)	0.8990(8)	2.7(3)
C8	0.5254(5)	0.1744(4)	0.9979(9)	3.7(4)
C9	0.5575(6)	0.3066(5)	1.0072(10)	4.4(4)
C10	0.4852(7)	0.3690(5)	1.0123(11)	5.3(5)
C11	0.3499(6)	0.4134(4)	0.9020(10)	4.1(4)
C12	0.2531(5)	0.3864(4)	0.9848(9)	3.5(4)
C13	0.1916(5)	0.2601(4)	1.0290(10)	2.9(4)
C14	0.5246(5)	0.0884(4)	0.6935(9)	3.5(4)
C15	0.4747(6)	0.0962(4)	0.5614(9)	4.0(4)
C16	0.3855(6)	0.1794(5)	0.4367(9)	4.4(4)
C17	0.3431(6)	0.2561(6)	0.4327(9)	4.5(5)
C18	0.2924(5)	0.2892(4)	0.6812(8)	3.3(4)
C19	0.2000(5)	0.3137(4)	0.7789(8)	2.8(4)
O1	0.4110(4)	−0.0257(3)	0.7959(6)	4.3(3)
O2	0.5098(4)	0.2425(3)	1.0774(6)	4.5(3)
O3	0.4272(4)	0.3603(3)	0.9002(6)	4.0(3)
O4	0.2001(4)	0.2678(3)	1.1554(6)	4.0(3)
O5	0.4363(4)	0.1701(3)	0.5559(6)	3.7(3)
O6	0.2625(4)	0.2714(3)	0.5472(6)	4.1(3)
N1	0.4550(4)	0.0932(3)	0.8264(7)	3.0(3)
N2	0.2176(4)	0.3156(3)	0.9302(7)	2.9(3)

$B_{iso} = (8\pi^2/3)\ \Sigma_i\Sigma_j U_{ij} a_i^* a_j^* (\boldsymbol{a}_i \cdot \boldsymbol{a}_j)$. Anisotropic thermal parameters and structure factors are available from the authors.

Results and discussion

Bond lengths, bond angles and torsional angles are given in Tables 2–4. In **1**, the ten intra-Cp ring C–C bond distances span the range 1.397(11) to 1.477(13) Å (av. 1.43(4) Å) and the ten internal Cp ring C–C–C bond angles the range 106.6(6) to 108.7(7)° (av. 108(1)°). The Ru–C bond distances over the range 2.169(7) to 2.194(7) Å (av. 2.18(1) Å). The five inter-Cp ring C–C closest contact distances span the range 3.595(10) to 3.645(11) Å (av. 3.62(3) Å), with the interplane distance between the Cp ring geometric centroids calculated as 3.62(1) Å. The Cp rings are, therefore, almost parallel, the dihedral angle between their least-squares planes being 1.1(4)°. This is very similar to the corresponding angle in the ferrocene analogue, which has been reported as 0.4° [3], and more recently re-determined as 1.1° [8]. Greater distortions within the metallocene have been observed for a ferrocene-containing cryptand in which the heterocyclic bridges are not equal in length [2]. In **1**, the carbons of substitution on each Cp ring are staggered by 73.7°. The Cp rings are removed slightly from eclipsed (D_{5h}) symmetry, with angular twists subtended by the five pairs of nearest eclipsed carbons spanning the range +0.26 to +2.97°, (av. +1.9°). The direction of this Cp inter-ring twist angle

Table 2

Bond lengths (Å), with esd's in parentheses

Ru–C1	2.189(7)	C5–C6	1.512(10)
Ru–C2	2.186(8)	C6–O1	1.225(10)
Ru–C3	2.194(7)	C6–N1	1.358(9)
Ru–C4	2.183(7)	C5′–C13	1.505(10)
Ru–C5	2.169(7)	C13–O4	1.220(11)
Ru–C1′	2.179(8)	C13–N2	1.372(10)
Ru–C2′	2.180(8)		
Ru–C3′	2.185(8)	N1–C14	1.460(9)
Ru–C4′	2.179(7)	C14–C15	1.510(13)
Ru–C5′	2.173(7)	C15–O5	1.429(9)
		O5–C16	1.414(10)
C1–C2	1.428(11)	C16–C17	1.495(13)
C2–C3	1.420(12)	C17–O6	1.452(10)
C3–C4	1.409(11)	O6–C18	1.418(10)
C4–C5	1.445(10)	C18–C19	1.517(10)
C5–C1	1.441(11)	C19–N2	1.479(10)
C1′–C2′	1.409(11)	N2–C12	1.477(9)
C2′–C3′	1.477(13)	C12–C11	1.517(11)
C3′–C4′	1.397(11)	C11–O3	1.422(9)
C4′–C5′	1.446(10)	O3–C10	1.419(11)
C5′–C1′	1.436(11)	C10–C9	1.491(12)
		C9–O2	1.434(10)
		O2–C8	1.430(10)
		C8–C7	1.503(11)
		C7–N1	1.476(9)

Table 3

Selected bond angles (°) with esd's in parentheses

C5–C1–C2	108.0(7)	C5–C6–O1	118.4(6)
C1–C2–C3	108.2(7)	C5–C6–N1	121.0(7)
C2–C3–C4	108.5(6)	O1–C6–N1	120.6(7)
C3–C4–C5	108.7(7)	C6–N1–C7	127.0(6)
C4–C5–C1	106.6(6)	C6–N1–C14	117.3(6)
C5′–C1′–C2′	107.7(7)	C7–N1–C14	115.6(5)
C1′–C2′–C3′	108.0(7)	C5′–C13–O4	120.7(7)
C2′–C3′–C4′	107.7(7)	C5′–C13–N2	117.4(7)
C3′–C4′–C5′	108.2(7)	O4–C13–N2	121.8(7)
C4′–C5′–C1′	108.4(6)	C13–N2–C19	125.0(6)
		C13–N2–C12	116.9(7)
C1–C5–C6	135.2(6)	C19–N2–C12	117.6(6)
C4–C5–C6	118.2(7)		
C1′–C5′–C13	134.1(7)	N2–C19–C18	110.5(6)
C4′–C5′–C13	117.5(7)	C19–C18–O6	106.3(6)
		C18–O6–C17	114.5(5)
N1–C7–C8	112.1(6)	O6–C17–C16	114.2(7)
C7–C8–O2	109.9(6)	C17–C16–O5	111.5(7)
C8–O2–C9	114.7(6)	C16–O5–C15	111.4(6)
O2–C9–C10	109.3(7)	O5–C15–C14	109.2(6)
C9–C10–O3	109.6(7)	C15–C14–N1	112.5(6)
C10–O3–C11	114.5(6)		
O3–C11–C12	112.7(6)		
C11–C12–N2	113.8(6)		

places the carbonyls at greater separation than would be the case for exactly eclipsed Cp rings.

The amide groups are both near-planar. For the amide containing the carbonyl C6=O1, angles about C6 and N1 total 360.0 and 359.9° respectively, whilst the four

Table 4

Selected torsion angles (°); esd's are ca. 1°

N1–C7–C8–O2	−174	O4–C13–N2–C12	−2
C7–C8–O2–C9	−87	C5′–C13–N2–C19	+3
C8–O2–C9–C10	+131	C5′–C13–N2–C19	+174
O2–C9–C10–O3	−82		
C9–C10–O3–C11	+175		
C10–O3–C11–C12	−93	H4′–C4′–C5′–C13	−2
O3–C11–C12–N2	−58	C4′–C5′–C13–O4	+37
C11–C12–N2–C19	−59	H4–C4–C5–C6	−1
C12–N2–C19–C18	+91	C4–C5–C6–O1	−15
N2–C19–C18–O6	+166		
C19–C18–O6–C17	+172	O4–C13–N2–C12	−2
C18–O6–C17–C16	+80	C13–N2–C12–H12B	+9
O6–C17–C16–O5	−69	O1–C6–N1–C14	−3
C17–C16–O5–C15	+179	C6–N1–C14–H14B	−40
C16–O5–C15–C14	−178		
O5–C15–C14–N1	+67		
C15–C14–N1–C7	−99	O1–C6–N1–C14	−3
C14–N1–C7–C8	−87	C5–C6–N1–C14	+178
		C5–C6–N1–C7	−2

torsion angles describing the amide C–N bond deviate from planarity by only 1.7 to 3.4°. The second amide is slightly more distorted; angles about C13 and N2 total 359.9 and 359.5° respectively, while the four torsion angles deviate from planarity by 2.2 to 6.7°. Although almost within the limits of accuracy, the more planar amide is observed to have greater C–N double bond character whilst lesser C=O double bond character. The more planar amide is therefore closer to the dipolar zwitterionic canonical form. The amides are largely coplanar with the Cp ring to which they are substituted, thus extending π-bonded delocalisation throughout each cyclopentadienyl-amido unit. This is more pronounced for the amide containing carbonyl C6=O1 (the more planar amide), since the four torsion angles defining the amide–Cp bond fall in the range 14.6 to 19.2°, whilst for the amide containing C13=O4 the corresponding torsion angles span 35.5 to 40.8°. The orientation of the carbonyls is *trans*, a feature now found to be general to this family of metallocenocryptands [2,3]. This minimises repulsion between the two C=O groups, and minimises the overall dipole moment of the molecule. The two carbonyls in **1** differ slightly in that C13=O4 is directed toward but C6=O1 away from the molecule's centre of mass. This feature is also observed in the ferrocene analogue.

The classes of bond lengths and angles and torsion angles describing the heterocyclic ring are substantially similar in kind to those reported for the ferrocene homologue. Six of the torsion angles are in the range 166–179°, eleven in the range 58–99° and one is intermediate at 131°. The heterocyclic rings for both analogues are therefore more or less equally puckered, with the diazacrown unit slightly more open in the ruthenocene analogue. The long non-bonded closest contact distance N1 ··· N2 in **1** is 5.147(8) Å, and reported as 5.220(10) Å in the ferrocene analogue [3]. These two distances are very similar despite the greater Cp ring separation in **1** which has to be bridged by bonds to nitrogen. This may indicate that it is the steric requirements of the heterocyclic diazacrown unit, rather than some energy minimum of metallocene Cp inter-ring twist, which are dominant in determining structure. Despite the fact that **1** contains no water of crystallization, its molecular structure closely resembles that of the ferrocene-containing analogue. This suggests that it is the covalent bonding which is decisive. Within the unit cell there are four molecules of **1**, which are in fact two pairs of mirror-image molecules. Therefore upon crystallisation no spontaneous resolution occurs, in contrast to the case of an asymmetric ferrocene-containing cryptand reported earlier for which the crystals were enantiomorphic [2].

The NMR spectra of **1** have been reported in detail [7], and the predicted structure of **1** has been confirmed by this X-ray study. The more deshielded of the Cp and heterocyclic ring ^{1}H nuclei are those residing spatially in the conical anisotropic deshielding zones of the carbonyls. Table 5 lists selected non-bonded closest contact distances. For **1** the non-bonded distances O1–H4, O1–H14B, O4–H4′ and O4–H12B are short, being 2.610(5), 2.410(5), 2.775(5) and 2.200(5) Å respectively, (H-atom numbering is that of the carbons to which they are bonded). It is these ^{1}H nuclei which are observed to resonate at low field. Thus, these data confirm the validity of the NMR assignments [7], and the observed Cp inter-ring twist in **1** re-inforces the molecular orbital description of d^6 metallocenes presented in this previous paper, for which ^{13}C NMR was employed as the probe.

The $Ru^{2+/3+}$ redox oxidation wave of **1** is observed at +1.1 V vs. SCE (MeCN as solvent with 0.1 *M* $^n Bu_4NClO_4$ as supporting electrolyte), but it is non-reversible

Table 5

Selected long non-bonding closest contact distances (Å) with esd's in parentheses

O1–H4	2.610(5)	C1–C5′	3.614(10)
		C2–C4′	3.610(11)
O1–H14A	3.685(5)	C3–C3′	3.645(11)
O1–H14B	2.410(5)	C4–C2′	3.644(11)
		C5–C1′	3.595(10)
O4–H4′	2.775(5)		
O4–H12A	3.332(5)		
O4–H12B	2.200(5)		
N1–N2	5.147(8)		

(i.e. little or no reduction wave is observed). For the corresponding ferrocene-containing analogue, the redox couple $Fe^{2+/3+}$ is observed at +0.62 V and is reversible [10]. For the complex of **1** with Dy^{3+}, the $Ru^{2+/3+}$ redox oxidation wave is observed to shift to +1.4 V, and is non-reversible. Shifts of this magnitude were observed for the ferrocene-containing analogue upon complex formation with similarly charge dense metal cations.

The electronic absorption spectrum of **1** in acetonitrile solution in the near UV consists of a broad band with $\lambda_{max} = 327(2)$ nm ($\epsilon = 530\ M^{-1}\ cm^{-1}$). For the 1:1 complex with Dy^{3+} one broad band is observed with $\lambda_{max} = 348(2)$ nm ($\epsilon = 780\ M^{-1}\ cm^{-1}$). This bathochromic shift with increased extinction co-efficient for **1** upon complexation with a metal cation mirrors the behaviour of the ferrocene analogue [11].

Acknowledgements

We thank RTZ Chemicals Ltd. and Rhône Poulene Chemicals for financial support (NWS).

References

1 I. Bernal, E. Raabe, G.M. Reisner, R.A. Bartsch, R.A. Holwerda, B.P. Czech and Z. Huang, Organometallics, 7 (1988) 247.
2 C.D. Hall, I.P. Danks, S.C. Nyburg, A.W. Parkins and N.W. Sharpe, Organometallics, 9 (1990) 1602.
3 P.D. Beer, C.D. Bush and T.A. Hamor, J. Organomet. Chem., 339 (1988) 133.
4 P.L. Bellon, F. Demartin, V. Scatturin and B. Czech, J. Organomet. Chem., 265 (1984) 65.
5 S. Akabori, S. Sato, T. Tokuda, Y. Habata, K. Kawazoe, C. Tamura and M. Sato, Chem. Lett., (1986) 121.
6 P.D. Beer, Chem. Soc. Rev., 18 (1989) 409.
7 C.D. Hall and N.W. Sharpe, Organometallics, 9 (1990) 952.
8 M.C. Grossel, M.R. Goldspink, J.A. Jriljac and S.C. Weston, personal communication; we are grateful to Dr. Grossel for permission to use as yet unpublished data.
9 E.J. Gabe, Y. Le Page, J.P. Charland, F.L. Lee and P.S. White, J. Appl. Crystallogr., 22 (1989) 384.
10 C.D. Hall, N.W. Sharpe, I.P. Danks and Y.P. Sang, J. Chem. Soc., Chem. Commun., (1989) 419.
11 C.D. Hall, I.P. Danks and N.W. Sharpe, J. Organomet. Chem., 390 (1990) 227.